

Selective growth of high quality GaN on Si(111) substrates

M. Seon, T. Prokofyeva, and M. Holtz^{a)}

Department of Physics, Texas Tech University, Lubbock, Texas 79409

S. A. Nikishin, N. N. Faleev, and H. Temkin

Department of Electrical Engineering, Texas Tech University, Lubbock, Texas 79409

(Received 27 September 1999; accepted for publication 4 February 2000)

We demonstrate selective growth of high-quality GaN by gas-source molecular beam epitaxy on Si(111) wafers patterned with SiO₂. GaN was grown on wafers having two different buffer layers. The first buffer layer contains two AlGaIn/GaN superlattices, separated by GaN spacer, grown on AlN, with a total thickness of 400 nm. The second is a thin AlN (1.5 nm) buffer layer. X-ray diffraction confirms (0001) growth orientation, smooth interfaces, and coherence lengths comparable to the layer thickness in both samples. In the case of the thin AlN buffer layer, the tensile stress measured by the E₂ Raman line shift is attributed to the mismatch in the thermal expansion coefficients of GaN and Si. However, when the AlGaIn/GaN superlattice buffer layer is grown first, a reduced stress is measured. High carrier concentrations ($\approx 10^{18} \text{ cm}^{-3}$) are seen in the GaN grown on the thin AlN buffer layer, which we attribute to the incorporation of silicon from the substrate during the growth process. The superlattice buffer layer is seen to inhibit this diffusion, resulting in a carrier concentration of $< 10^{17} \text{ cm}^{-3}$ in the GaN. © 2000 American Institute of Physics. [S0003-6951(00)01214-6]

GaN is an important wide band gap semiconductor due to numerous applications in electronics and optoelectronics.^{1,2} GaN is generally grown on sapphire or silicon carbide substrates. However, it would be highly advantageous to grow GaN on silicon substrates³⁻⁶ due to potential integration between GaN high power electronics and silicon technologies. Stress, ubiquitous due to lattice mismatch (17%) between Si and GaN and due to differences in their thermal expansion coefficients, is critical because it causes dislocations and even cracking. We have recently demonstrated that high quality GaN can be deposited on Si(111) without cracks, provided an AlN buffer layer and a short-period AlGaIn/GaN superlattice (SL) is grown prior to the GaN.⁷ We find this to be superior to GaN grown with only an AlN buffer layer.

This work describes the preparation of high quality GaN on Si(111) when the substrate wafers are patterned with SiO₂, to produce “windows” of exposed Si surrounded by the oxide “mask.” Two different buffer layers are studied. The first buffer layer is identical to what we used previously to demonstrate high quality GaN on Si(111).⁷ The second buffer layer is thin AlN, which inhibits SiN_x formation at the substrate interface, provides coalesced growth islands of AlN which are well oriented and provide a smooth surface for the GaN. We use atomic force microscopy (AFM), triple-crystal x-ray diffraction (XRD), and Raman spectroscopy to demonstrate that high quality GaN is deposited in the window regions. We find that GaN also forms on the oxide mask, with poorer properties.

The growth experiments were carried out on Si(111) wafers having a 2 in. diameter. Thermal oxide was grown on the wafers at 1100 °C to a thickness of $\approx 200 \text{ nm}$. The oxide was patterned using photolithography into large window

fields, ranging in width and length from 0.2 to 10 mm. A final wet etch step was used to ensure hydrogen terminated surfaces of the silicon in the window regions.⁸ Nitride deposition followed using gas-source molecular beam epitaxy (GSMBE) with ammonia. Growth was initiated by exposing the wafer surfaces to Al,⁹ followed by exposure to ammonia.¹⁰ Repeating this procedure 5–10 times suppresses the formation of silicon nitride islands on the silicon window¹¹ and form a well-oriented template for subsequent growth of GaN and AlGaIn. A cross-sectional diagram of the sample is shown in the inset to Fig. 1. The buffer layer of sample A consists of a 60 nm AlN layer, followed by two AlGaIn/GaN superlattices (each SL 45 nm thick separated by 250 nm of GaN).¹² This approach has been used to demonstrate growth of GaN with excellent crystal quality using MBE⁷ and metalorganic chemical vapor deposition.¹² The final GaN epilayer of sample A was $\approx 0.5 \mu\text{m}$ thick. The buffer layer of sample B was thin AlN ($\approx 1.5 \text{ nm}$). The GaN epilayer of sample B was $\approx 1.0 \mu\text{m}$ thick, so that both

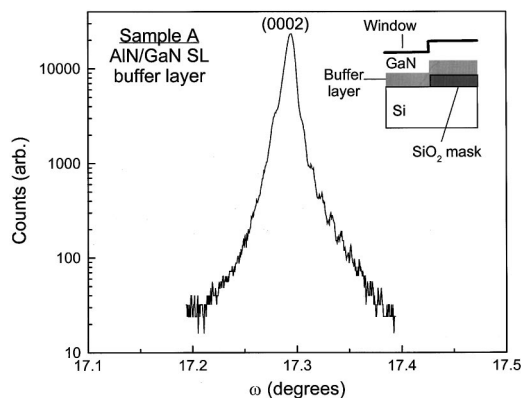


FIG. 1. A 2θ - ω diffraction pattern of the GaN (0002) peak on sample with AlGaIn/GaN superlattice buffer layer. The inset diagrams the sample.

^{a)}Electronic mail: Mark.Holtz@ttu.edu

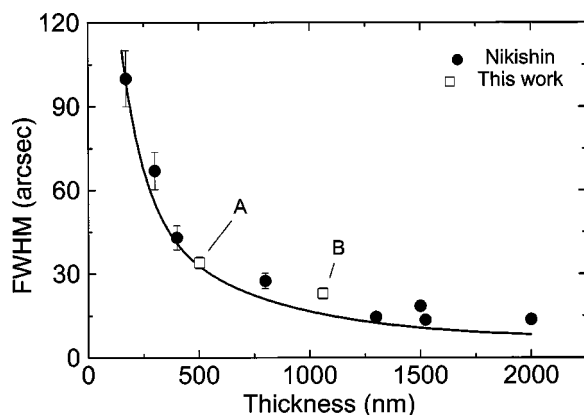


FIG. 2. Open squares are XRD linewidths (FWHM) of the GaN (0002) peak. Closed circles are data from uniform GaN films on Si(111), and the curve is calculated FWHM vs thickness for ideal crystalline layers.⁷

samples have comparable total thickness. Both GaN layers were grown at 1000 ± 30 K.

In situ reflection high-energy electron diffraction (RHEED) confirmed uniform coverage by the buffer layer over the window region for both samples. For sample A, the GaN growth mode on the buffer layer was two-dimensional with a 2×2 surface structure. For sample B, three-dimensional growth was seen during the formation of the first islands of GaN. After five minutes of growth we observed a mixture of 1×1 and 2×2 surface structures of GaN. After seven minutes we saw 2×2 surface structure which corresponds to two-dimensional growth of GaN. Deposition of GaN also takes place over the oxide mask. The SL buffer layer of sample A provided uniform oxide coverage. In contrast, the thin AlN buffer layer of sample B resulted in AlN islands on the oxide, with incomplete coverage.

XRD from the window regions of samples A and B exhibited only the (0002) and (0004) reflections, confirming that the GaN was grown in the $c=[0001]$ direction. A 2θ - ω diffraction pattern of the GaN (0002) peak on sample A is shown in Fig. 1. The sharpness of the (0002) peak demonstrates high crystalline quality and the presence of Pendellösung fringes confirm flatness of the GaN surface and a smooth interface with the buffer layer. This is in good agreement with AFM surface topography measurements. In both samples we find ≈ 7 – 8 nm root-mean-square (rms) roughness of the GaN over the window regions ($20 \mu\text{m} \times 20 \mu\text{m}$ scan range). XRD 2θ - ω diffraction measurements of the (0002) peak from sample B showed a similarly narrow line.

The (0002) peak full width at half maximum (FWHM), as a function of the layer thickness, is shown in Fig. 2 (open squares). For comparison, the data from Ref. 7, together with their curve calculated for ideal crystalline layers¹³ as a function of thickness, are included. The good agreement between measured and calculated FWHM shows that GaN layers of samples A and B have good crystal perfection with vertical block size comparable to the total layer thickness. The measured FWHM is greater than the theoretical value for sample B because of the three-dimensional growth in the early epitaxy stage. This results in an x-ray coherence length smaller than the total thickness of the layer.

Figure 3 shows Raman spectra from samples A and B,

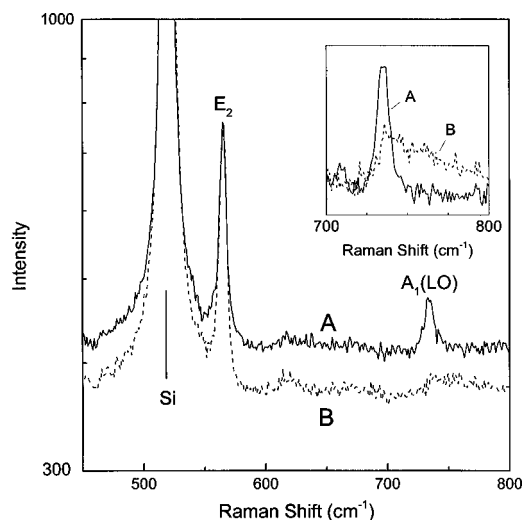


FIG. 3. Raman spectra (room temperature, $\lambda_L = 514.5$ nm) of each sample well inside the window regions. The inset shows higher S/N acquisition of the $A_1(\text{LO})$ region.

both taken from the window regions. A logarithmic intensity scale is used. The band at 520 cm^{-1} is the Si substrate $\text{O}(\Gamma)$ phonon. Near 566 cm^{-1} is the E_2 (high) band from GaN, and at 735 cm^{-1} we observe the $A_1(\text{LO})$ phonon. The presence of these two bands is consistent with c -axis backscattering,¹⁴ confirming, along with the XRD data, that the GaN hexagonal structure $[0001]$ crystal axis is parallel to the Si $[111]$ direction.

Figure 3 (and the inset) shows a reduction in the $A_1(\text{LO})$ band intensity in sample B. For undoped material, the $A_1(\text{LO})$ to E_2 relative intensity should be $\approx 1:3$.¹⁵ When free-carriers are present the plasma interacts with the $A_1(\text{LO})$ phonon, resulting in a mixed phonon-plasmon mode. The mixed modes gain intensity at the expense of the $A_1(\text{LO})$ phonons¹⁶ and blue shift with increasing carrier concentration. Along with the intensity reduction of the $A_1(\text{LO})$, the higher coupled plasmon-phonon band (L_+) is observed at higher energy than $A_1(\text{LO})$. For sample A we estimate a carrier concentration to be $< 10^{17} \text{ cm}^{-3}$ based on the $A_1(\text{LO})$ to E_2 relative intensity. Capacitance-voltage measurements support these estimates.¹⁷ For sample B we observe a reduced intensity, a blueshift, and broadening. We estimate the carrier concentration to be $\approx 10^{18} \text{ cm}^{-3}$ based on the $A_1(\text{LO})$ -plasmon coupled mode peak energy¹⁸ and the $A_1(\text{LO})$ to E_2 relative intensities. We observe higher carrier concentrations ($> 10^{18} \text{ cm}^{-3}$) in the GaN over our mask regions, as well.

Elevated carrier concentrations can stem from two effects: Incorporation of dopant species and the presence of native point defects, such as vacancies. It has been previously seen that the substrate can be a source for dopant atoms in GaN grown over SiO_2 .^{19–21} In the present case of GaN in the window region, a plausible source for free-carriers is out diffusion of silicon from the substrate during the growth process, as reported in Ref. 22. Sample A has a much weaker impurity incorporation from this effect than sample B. We conclude that the AlGaIn/GaN SL buffer layer in sample A acts as an impurity diffusion barrier, in agreement with Ref. 7. This can be attributed simply to the different buffer layers of samples A and B. Transmission electron

micrographs show threading dislocation walls, which originate near the silicon substrate, and propagate upward through the nitride layer to the SL. Beyond the SL, the threading dislocation density is drastically reduced (i.e., grain sizes increase). This, combined with the low free-carrier concentration detected in sample A, lead us to suggest that the threading dislocation walls enhance Si diffusion into the GaN. The thin AlN buffer layer is not an effective impurity diffusion barrier. Perhaps this is because the grain size remains small during the early phases of the growth, as seen from the RHEED measurements. In addition, the diffusing impurity is believed to be silicon. Prior work dealt with GaN grown over SiO₂, in which case Si was suspected but O could not be ruled out.^{19,21} In our present case, oxygen atoms are unlikely to diffuse into the GaN above the window regions in sufficiently large quantities to cause the doping effect we observe.

The E₂ Raman band is known to shift with stress.^{23,24} Our average of 25 measurements within the window region (far from the window/mask edge) of sample A give an E₂ shift of $-2.6 \pm 0.1 \text{ cm}^{-1}$ corresponding to a tensile stress of $0.34 \pm 0.05 \text{ GPa}$.²⁴ Stress shifts the E₂ phonon of sample B (far from the mask edge) by $-3.1 \pm 0.1 \text{ cm}^{-1}$. This implies a tensile stress of $0.40 \pm 0.06 \text{ GPa}$.

The tensile stress on the GaN epilayer in the window region is mainly due to the thermal expansion mismatch between the GaN epilayer and the substrate. The thermal expansion coefficients ($\alpha = \partial \ln a / \partial T$) of the respective materials are $3.59 \times 10^{-6} \text{ K}(\text{Si})$ and $5.59 \times 10^{-6} \text{ K}(\text{GaN} \perp c \text{ axis})$.²⁵ Using these values, the Young's modulus (E) and Poisson ratio (ν) from Ref. 26, and $\epsilon_a = (\sigma_a/E)(1 - \nu)$ we calculate the tensile stress σ_a in the GaN due to the α mismatch with Si to be 0.39 GPa. The measured values are within error of each other, and that calculated based on expansion coefficient mismatch. However, most of the error bar comes from the stress-shift calibration,²⁴ and less than $\pm 0.01 \text{ GPa}$ comes from the phonon energy variation. The Raman data show that the stress is greater in the window region of sample B than A. We conclude that the stress in sample B is attributable to the expansion mismatch between GaN and Si, with the thin AlN buffer layer playing a negligible role. The smaller measured value in the window region of sample A is attributed to the presence of the SL buffer layer.

In summary, we have demonstrated GSMBE growth of GaN on patterned silicon substrates. We show that high quality GaN grows selectively in the window regions. Based on AFM, both samples show good surface morphology. XRD and Raman confirm [0001]-oriented crystal growth. The crystal quality is comparable to that of our previous GaN uniformly deposited on Si(111) wafers. Raman scattering exhibited narrow E₂ phonon bands. Based on the E₂ phonon redshift, the tensile stress on the GaN is found to be due primarily to differences in the thermal expansion coefficients of GaN and Si. Agreement between the measured and calculated stress is best for sample B (thin AlN buffer layer). A measurable phonon shift, corresponding to partial stress re-

laxation, is observed in sample A, due to the presence of the SL buffer layer. In addition, we believe the SL buffer layer to serve as a diffusion barrier to silicon incorporation in the GaN.

This research was supported by AFOSR (Major Dan Johnstone), DARPA (Dr. R. F. Leheny) and the J. F. Maddox Foundation. The authors wish to thank Vladimir Antipov and Rusty Harris for patterning the substrate.

- ¹S. Nakamura, in *Semiconductors and Semimetals*, Vol. 50, edited by J. I. Pankove and T. D. Moustakas (Academic, San Diego, 1998), p. 431.
- ²S. J. Pearton, J. C. Zolper, R. J. Shul, and F. Ren, *J. Appl. Phys.* **86**, 1 (1999).
- ³K. S. Stevens, M. Kinniburgh, and R. Beresford, *Appl. Phys. Lett.* **66**, 3518 (1995).
- ⁴S. Guha and N. A. Bojarczuk, *Appl. Phys. Lett.* **72**, 415 (1998).
- ⁵D. Kuksenkov, H. Temkin, R. Gaska, and J. W. Yang, *IEEE Electron Device Lett.* **19**, 222 (1998).
- ⁶H. Marchand, N. Zhang, L. Zhao, Y. Golan, S. J. Rosner, G. Girolami, P. T. Fini, J. P. Ibbetson, S. Keller, S. DenBaars, J. S. Speck, and U. K. Mishra, *MRS Internet J. Nitride Semicond. Res.* **4**, 2 (1999) and references therein.
- ⁷S. A. Nikishin, N. N. Faleev, V. G. Antipov, S. Francoeur, L. Grave de Peralta, G. A. Seryogin, H. Temkin, T. I. Prokofyeva, M. Holtz, and S. N. G. Chu, *Appl. Phys. Lett.* **75**, 2073 (1999).
- ⁸V. G. Antipov, S. A. Nikishin, and D. V. Sinyavskii, *Tech. Phys. Lett.* **17**, 45 (1991).
- ⁹E. Calleja, M. A. Sánchez-García, F. J. Sánchez, F. Calle, F. B. Naranjo, E. Muñoz, S. I. Molina, A. M. Sánchez, F. J. Pacheco, and R. García, *J. Cryst. Growth* **201/202**, 296 (1999).
- ¹⁰S. A. Nikishin and H. Temkin (unpublished).
- ¹¹S. A. Nikishin, V. G. Antipov, S. Francoeur, N. N. Faleev, G. A. Seryogin, V. A. Elyukhin, H. Temkin, T. I. Prokofyeva, M. Holtz, A. Konkar, and S. Zollner, *Appl. Phys. Lett.* **75**, 484 (1999).
- ¹²X. Zhang, S.-J. Chua, P. Li, K.-B. Chong, and Z.-C. Feng, *Appl. Phys. Lett.* **74**, 1984 (1999).
- ¹³S. Takagi, *Acta Crystallogr.* **15**, 1311 (1962).
- ¹⁴N. Grandjean, J. Massies, P. Vennéguès, M. Leroux, F. Demangeot, M. Renucci, and J. Frandon, *J. Appl. Phys.* **83**, 1379 (1998).
- ¹⁵T. Kozawa, T. Kachi, H. Kano, Y. Taga, M. Hashimoto, N. Koide, and K. Manabe, *J. Appl. Phys.* **75**, 1098 (1994).
- ¹⁶P. Perlin, J. Camassel, W. Knap, T. Taliercio, J. C. Chervin, T. Suski, I. Grzegory, and S. Porowski, *Appl. Phys. Lett.* **67**, 2524 (1995).
- ¹⁷T. Prokofyeva and V. Veena (unpublished).
- ¹⁸H. Harima, K. Sakashita, and S. Nakashima, *Mater. Sci. Forum* **264-268**, 1363 (1998).
- ¹⁹A. Kaschner, A. Hoffmann, C. Thomsen, F. Bertram, T. Riemann, J. Christen, K. Hiramatsu, T. Shibata, and N. Sawaki, *Appl. Phys. Lett.* **74**, 3320 (1999).
- ²⁰We also observe increased free-carrier concentration in the GaN deposited on the oxide mask region.
- ²¹M. Holtz, M. Seon, T. Prokofyeva, H. Temkin, R. Singh, F. P. Dabrowski, and T. D. Moustakas, *Appl. Phys. Lett.* **75**, 1757 (1999).
- ²²M. A. Sánchez-García, E. Calleja, F. J. Sánchez, F. Calle, E. Monroy, D. Basak, E. Muñoz, C. Villar, A. Sanz-Hervas, M. Aguilar, J. J. Serrano, and J. M. Blanco, *J. Electron. Mater.* **27**, 276 (1998).
- ²³C. Kieselowski, J. Krüger, S. Ruminov, T. Suski, J. W. Ager III, E. Jones, Z. Liliental-Weber, M. Rubin, E. R. Weber, M. D. Bremser, and R. F. Davis, *Phys. Rev. B* **54**, 17 745 (1996).
- ²⁴I. Lee, I. Choi, C. Lee, E. Shin, D. Kim, S. Noh, S. Son, K. Lim, and H. Lee, *J. Appl. Phys.* **83**, 5787 (1998).
- ²⁵J. Wang, R. S. Qhalid Fareed, M. Hao, S. Mahanty, S. Tottori, Y. Ishikawa, T. Sugahara, Y. Morishima, K. Nishino, M. Osinski, and S. Sakai, *J. Appl. Phys.* **85**, 1895 (1999).
- ²⁶T. Kozawa, T. Kachi, H. Kano, H. Nagase, N. Koide, and K. Manabe, *J. Appl. Phys.* **77**, 4389 (1995).